Relativistic Corrections in Atoms and Space-Time Variation of the Fine Structure Constant

Vladimir A. Dzuba, Victor V. Flambaum, Michael T. Murphy, and John K. Webb

School of Physics, University of New South Wales, UNSW Sydney NSW 2052, Australia

Abstract. Comparison of quasar absorption line spectra with laboratory spectra provides the best probe for variability of the fine structure constant, $\alpha = e^2/\hbar c$, over cosmological time-scales. We have demonstrated [1] that high sensitivity to the variation of α can be obtained from a comparison of the spectra of heavy and light atoms and have obtained an order of magnitude gain in precision over previous methods [2]. Our new data [3] hint that α was smaller at earlier epochs. Careful searches have so far not revealed any spurious effect that can explain the observations.

1 Introduction

Theories unifying gravity and other interactions suggest the possibility of spatial and temporal variation of physical "constants" in the Universe (see, e.g. [4]). Current interest is high because in superstring theories – which have additional dimensions compactified on tiny scales – any variation of the size of the extra dimensions results in changes in the 3-dimensional coupling constants. At present no mechanism for keeping the internal spatial scale static has been found (for example, our three "large" spatial dimensions increase in size). Therefore, unified theories applied to cosmology suffer generically from a problem of predicting time-dependent coupling constants. Moreover, there exists a mechanism for making all coupling constants and masses of elementary particles both space and time dependent, and influenced by local circumstances [5]. The variation of coupling constants can be non-monotonic (for example, damped oscillations).

Astrophysical measurements enable us to probe the variation of the fundamental constants. The energy scale of atomic spectra is given by the atomic unit $me^4/\hbar^2$. In the non-relativistic limit, all atomic spectra are proportional to this constant and analyses of quasar spectra cannot detect any change of the fundamental constants. Indeed, any change in the atomic unit will be absorbed in the determination of the redshift parameter z ($1 + z = \omega/\omega'$, ω' is the redshifted frequency of the atomic transition and ω is the laboratory value). However, any change in the fundamental constants can be found by measuring the relative size of relativistic corrections, which are proportional to α^2.

It is natural to search for any changes in α using measurements of the spin-orbit splitting within a specific fine structure multiplet. Indeed, this method has

been applied to quasar spectra by several groups. The ratio of fine structure splitting of an alkali-type doublet to the mean transition frequency is proportional to α^2. A comparison of these ratios in cosmic spectra with laboratory values provides powerful constraints on variability. This method was proposed by J. Bachall and M. Schmidt in 1967 [6]. Varshalovich, Panchuk & Ivanchik [7] have obtained very stringent upper limits on any variation at redshifts $z \sim 2.8$–3.1 at the fractional level of $\Delta\alpha/\alpha \equiv (\alpha_z - \alpha_0)/\alpha_0 = 0.2 \pm 0.7 \times 10^{-4}$. Here, α_0 is the present day value of α and α_z is the value at the redshift, z, of the absorbing gas cloud. See [8] for a review of other works.

Recently we developed a new approach which improves the sensitivity to a variation of α by more than an order of magnitude [1,2]. The relative value of any relativistic corrections to atomic transition frequencies is proportional to α^2. These corrections can exceed the fine structure interval between the excited levels by an order of magnitude (for example, an s-wave electron does not have the spin-orbit splitting but it has the maximal relativistic correction to energy). The relativistic corrections vary very strongly from atom to atom and can have opposite signs in different transitions (for example, in s-p and d-p transitions). Thus, any variation of α could be revealed by comparing different transitions in different atoms in cosmic and laboratory spectra.

This method provides an order of magnitude precision gain compared to measurements of the fine structure interval. Relativistic many-body calculations are used to reveal the dependence of atomic frequencies on α for a range of atomic species observed in quasar absorption spectra [1]. It is convenient to present results for the transition frequencies as functions of α^2 in the form

$$\omega = \omega_0 + q_1 x + q_2 y, \tag{1}$$

where $x = (\frac{\alpha}{\alpha_0})^2 - 1$, $y = (\frac{\alpha}{\alpha_0})^4 - 1$ and ω_0 is a laboratory frequency of a particular transition. New and accurate laboratory measurements of ω_0 have been carried out specifically for this work by Imperial College (London), Lund and NIST groups (see also accurate measurements in [9,10,12,13,14,15] [16,17,18,19]). We stress that the second and third terms contribute only if α deviates from the laboratory value α_0. The initial observational results [2] for two MgII lines and five FeII lines suggest that α may have been smaller in the past.

This work has been continued in Ref. [3]. A large set of data consists of 49 quasar absorption systems located between 4 and 11 billion light years from us (starting from 10% of the age of the Universe after Big Bang). Many lines of MgI, MgII, AlII, AlIII, SiII, CrII, FeII, NiII and ZnII have been included and a study of both temporal and spatial dependence of α has been performed. For the whole sample, $\Delta\alpha/\alpha = (-7.5 \pm 1.8) \times 10^{-6}$. We should stress that only statistical errors are presented here. This error is now small and the main efforts are directed towards the study of various systematic effects [20].

Note that the data have already passed one crucial test. The relativistic corrections vary very strongly from atom to atom and can have opposite signs in different transitions (for example, in s-p and d-p transitions). It is hard to imagine that the spurious effects "know" about this. Therefore, we measured α

variation separately for positive shifters (positive coefficient q_1 in eq. (1)) combined with anchor lines (small q_1) and negative shifters combined with anchor lines. Startlingly, the results for $\Delta\alpha$ are the same in both cases! Spurious shifts of the lines would give the opposite signs for "$\Delta\alpha$" in these two cases.

This cosmic spectroscopy method has been extended to study variation of other fundamental parameters. The ratio of the hydrogen atom hyperfine transition frequency to a molecular (CO, CN, CS, HCO^+, HCN etc.) rotational frequency is proportional to $y = \alpha^2 g_p$ where g_p is the proton magnetic g-factor [21]. A new preliminary result here is $\Delta y/y = (-2.4 \pm 1.8) \times 10^{-6}$ about 4 billion light years from us (the average z=0.47). Altogether, we now have 3 independent samples of data: two optical samples (see [2,3]) and one radio sample. All 3 samples hint that $\Delta\alpha$ is negative.

Another possibility is to use optical atomic frequency standards. Any evolution of α in time would lead to a frequency shift. To establish the connection between $\dot{\alpha}$ and $\dot{\omega}$, relativistic calculations of the α dependence of the relevant frequencies for CaI, SrII, BaII, YbII, HgII, InII, TlII and RaII have been performed [1]. The α dependence of the microwave frequency standards (Cs, Hg^+) has also been accurately calculated.

2 Atomic Theory

2.1 Semi-Empirical Estimations and Advantages of the New Method to Search for Variation of α

To explain the advantages of our proposals let us start from simple analytical estimates of the relativistic effects in transition frequencies. The contribution of the relativistic correction to the energy can be obtained as an expectation value $\langle V \rangle$ of the relativistic perturbation V, which is large in the vicinity of the nucleus only. The wave function of an external electron near the nucleus is presented in, for example, [22]. A simple calculation of the relativistic correction to the energy of external electron gives the following result:

$$\begin{aligned} \Delta_n &= -\frac{me^4 Z_a^2}{2\hbar^2} \frac{(Z\alpha)^2}{\nu^3} \left[\frac{1}{j+1/2} - C(j,l) \right] \\ &= \frac{E_n (Z\alpha)^2}{\nu} \left[\frac{1}{j+1/2} - C(j,l) \right], \end{aligned} \tag{2}$$

where Z is the nuclear charge, l and j are the orbital and total electron angular momenta, Z_a is the charge "seen" by the external electron outside the atom, i.e. $Z_a = 1$ for neutral atoms, $Z_a = 2$ for singly charged ions, etc.; ν is the effective principal quantum number, defined by $E_n = -\frac{me^4}{2\hbar^2}\frac{Z_a^2}{\nu^2}$, where E_n is the energy of the electron. For hydrogen-like ions $\nu = n, Z_a = Z$, where n is the principal quantum number. To describe the contribution of many-body effects to the relativistic correction, Δ_n, we introduce the parameter $C(j,l)$. Indeed, the single-particle relativistic correction increases the attraction of an

electron to the nucleus and makes the radius of the electron cloud smaller. As a result, the atomic potential, which is the nuclear potential screened by the core electrons, becomes weaker. This decreases the binding energy of the external electron. Therefore, the many body effect has the opposite sign to the direct single-particle relativistic effect. Accurate many-body calculations described below give $C(j,l) \sim 0.6$ for s and p orbitals. We see that the relativistic correction is largest for the $s_{1/2}$ and $p_{1/2}$ states, where $j = 1/2$. The fine structure splitting is given by $\Delta_{ls} = E(p_{3/2}) - E(p_{1/2})$.

In quasar absorption spectra, transitions from the ground state are most commonly seen. Therefore, it is important to understand how the frequencies of these transitions are affected by the relativistic effects. The fine splitting in excited states is smaller than the relativistic correction in the ground state since the density of the excited electron near the nucleus is smaller. As a result, the fine splitting of the $E1$-transition from the ground state (e.g., s–p) is substantially smaller than the absolute shift of the frequency of the s–p transition. At $C(j,l) = 0.6$ the relativistic shift of the mean energy of the p-electron ($E(p) = 2/3E(p_{3/2}) + 1/3E(p_{1/2})$) is small. Therefore, the average relativistic shift of the s-p transition frequency is mostly given by the energy shift of the s-state: $\Delta(p\text{–}s) \simeq -\Delta(s)$.

The relative size of the relativistic corrections is proportional to Z^2, so they are small in light atoms. Therefore, we can find the change of α by comparing transition frequencies in heavy and light atoms or by comparing s-p and d-p transitions in heavy atoms (like FeII and CrII) where the relativistic frequency shifts have opposite signs.

We stress that the most accurate and effective procedure to search for the change of α must include the analysis of all available lines (rather than the fine splitting in the excited states within one multiplet only). This new method has the following advantages:

- The total relativistic shift of frequencies (e.g. the largest s-electron shift) is included.
- The largest relativistic shift in the ground state is included.
- Very large statistics – all available atomic and ionic lines, different frequency ranges, different redshifts (epoch/distances).
- Many possibilities to search for systematic errors. For example, we can exclude any line or atom to avoid possible effects of unknown line blending, calibration errors, etc. The opposite signs and different values of the relativistic shifts for different lines give us a very efficient method to control the systematic effects.

As a result we can measure the effect which is ∼10 times larger than that in the alkali doublet method, have ∼100 larger statistics, cover a large range of red-shifts/cosmological time and have better control of the systematic errors.

2.2 Relativistic Many-Body Calculations

Accurate calculations of relativistic effects in atoms have been done using many-body theory which includes electron-electron correlations. We used a correlation-

Table 1. Dependence on α of the frequencies of the $E1$ atomic transitions of astronomic interest; Z = 6 - 13 (units: cm^{-1}). Here $\omega = \omega_0 + q_1 x + q_2 y$ where $x = (\frac{\alpha}{\alpha_l})^2 - 1, y = (\frac{\alpha}{\alpha_l})^4 - 1$

Z	Atom/Ion	Ground state		Upper states		ω_0	q_1	q_2
6	C I	$2s^22p^2$	$^3P_0$	$2s^22p3s$	$^3P_1$	60352.642 [18]	9	0
				$2s2p^3$	$^3D_1$	64089.861 [18]	143	0
				$2s2p^3$	$^3P_1$	75253.984 [18]	70	0
				$2s^22p4s$	$^3P_1$	78116.743 [18]	29	0
				$2s^22p3d$	$^3D_1$	78293.490 [18]	52	0
6	C II	$2s^22p$	$^2P^o_{1/2}$	$2s2p^2$	$^2D_{3/2}$	74932.617 [18]	177	3
				$2s2p^2$	$^2S_{1/2}$	96493.742 [18]	171	3
				$2s2p^2$	$^2P_{1/2}$	110625.1 [19]	173	-3
				$2s2p^2$	$^2P_{3/2}$	110666.3 [19]	217	3
6	C IV	$1s^22s$	$^2S_{1/2}$	$1s^22p$	$^2P_{1/2}$	64484.094 [18]	108	8
				$1s^22p$	$^2P_{3/2}$	64591.348 [18]	231	-8
7	N V	$2s$	$^2S_{1/2}$	$2p$	$^2P_{1/2}$	80463.211 [18]	196	-4
				$2p$	$^2P_{3/2}$	80721.906 [18]	488	2
8	O I	$2p^4$	$^3P_2$	$2p^33s$	$^3S_1$	76794.977 [18]	130	-30
				$2p^34s$	$^3S_1$	96225.055 [18]	140	-20
12	Mg I	$3s^2$	$^1S_0$	$3s3p$	$^1P_1$	35051.264(1) [14]	106	-10
12	Mg II	$3s$	$^2S_{1/2}$	$3p$	$^2P_{1/2}$	35669.298(2) [14]	120	0
				$3p$	$^2P_{3/2}$	35760.848(2) [14]	211	0
13	Al II	$3s^2$	$^1S_0$	$3s3p$	$^1P_1$	59851.972(4) [15]	270	0
13	Al III	$3s$	$^2S_{1/2}$	$3p$	$^2P_{1/2}$	53682.880(2) [15]	216	0
				$3p$	$^2P_{3/2}$	53916.540(1) [15]	464	0

potential (self-energy operator) method [23] for atoms with one external electron above closed shells and a combined configuration interaction and many-body perturbation theory method [24] for atoms with several valence electrons. These *ab initio* methods allow us to obtain an accuracy of $\sim 0.1\%$ for energy levels in atoms and ions with one external electron above closed shells and a few per cent in atoms with several valence electrons. The accuracy was controlled by comparison between the calculated and observed energy levels and fine structure intervals. The values of the relativistic corrections and coefficients (q_1 and q_2) were obtained by repeating the calculations for different values of α (see eq. (1)).

The numerical procedure is the following:

- A relativistic Hartree-Fock (RHF) Hamiltonian was used to generate a complete set of single-electron orbitals, energy levels and Green's functions.
- Many-body perturbation theory in difference between the exact and Hartree-Fock Hamiltonians (perturbation $U = H - H_{HF}$) is used to calculate the effective Hamiltonian for valence electrons. This effective Hamiltonian includes correlations between the valence and core electrons which result in

Table 2. Same as Table I; Z = 14 - 25

Z	Atom/Ion	Ground state	Upper states	ω_0	q_1	q_2
14	Si II	$3s^2 3p\ ^2\mathrm{P}^o_{1/2}$	$3s3p^2\ ^4\mathrm{P}_{1/2}$	42824.297 [18]	437	10
			$3s3p^2\ ^4\mathrm{P}_{3/2}$	42932.625 [18]	543	13
			$3s3p^2\ ^2\mathrm{D}_{3/2}$	55309.3365(4) [15]	547	-6
			$3s^24s\ ^2\mathrm{S}_{1/2}$	65500.4492(7) [15]	24	22
			$3s3p^2\ ^2\mathrm{S}_{1/2}$	76665.352 [18]	558	-22
			$3s^23d\ ^2\mathrm{D}_{3/2}$	79338.501 [18]	298	-3
			$3s3p^2\ ^2\mathrm{P}_{1/2}$	83801.947 [18]	505	13
			$3s3p^2\ ^2\mathrm{P}_{3/2}$	84004.261 [18]	724	3
14	Si IV	$2p^63s\ ^2\mathrm{S}_{1/2}$	$2p^63p\ ^2\mathrm{P}_{1/2}$	71287.523 [18]	362	-8
			$2p^63p\ ^2\mathrm{P}_{3/2}$	71748.625 [18]	766	48
20	Ca I	$4s^2\ \ ^1\mathrm{S}_0$	$4s4p\ \ ^1\mathrm{P}_1$	23652.305 [18]	300	0
20	Ca II	$3p^64s\ ^2\mathrm{S}_{1/2}$	$3p^64p\ ^2\mathrm{P}_{1/2}$	25191.512 [18]	192	16
			$3p^64p\ ^2\mathrm{P}_{3/2}$	25414.427 [18]	420	16
24	Cr II	$3d^5\ \ ^6\mathrm{S}_{5/2}$	$3d^44p\ ^6\mathrm{F}_{3/2}$	46905.17 [17]	-1624	-25
			$3d^44p\ ^6\mathrm{F}_{5/2}$	47040.35 [17]	-1493	-21
			$3d^44p\ ^6\mathrm{F}_{7/2}$	47227.24 [17]	-1309	-18
			$3d^44p\ ^6\mathrm{P}_{3/2}$	48398.868(2) [16]	-1267	-9
			$3d^44p\ ^6\mathrm{P}_{5/2}$	48491.053(2) [16]	-1168	-16
			$3d^44p\ ^6\mathrm{P}_{7/2}$	48632.055(2) [16]	-1030	-13
25	Mn II	$3d^54s\ ^7\mathrm{S}_3$	$3d^54p\ ^7\mathrm{P}_2$	38366.184 [18]	918	34
			$3d^54p\ ^7\mathrm{P}_3$	38543.086 [18]	1110	19
			$3d^54p\ ^7\mathrm{P}_4$	38806.664 [18]	1366	27

Table 3. Same as Tables 1 and 2; Z = 26

Z	Atom/Ion	Ground state	Upper states	ω_0	q_1	q_2
26	Fe II	$3d^64s\ z\ ^6\mathrm{D}_{9/2}$	$3d^64p\ ^6\mathrm{D}^o_{9/2}$	38458.9871(2) [10]	1449	2
			$3d^64p\ z\ ^6\mathrm{D}^o_{7/2}$	38660.0494(2) [10]	1687	-36
			$3d^64p\ z\ ^6\mathrm{F}_{11/2}$	41968.0642(2) [10]	1580	29
			$3d^64p\ z^6\mathrm{F}_{9/2}$	42114.8329(2) [10]	1730	26
			$3d^64p\ z\ ^6\mathrm{F}_{7/2}$	42237.0500 [10]	1852	26
			$3d^64p\ z\ ^6\mathrm{P}_{7/2}$	42658.2404(2) [10]	1325	47
			$3d^64p\ z\ ^4\mathrm{F}_{9/2}$	44232.512 [18]	936	278
			$3d^64p\ z\ ^4\mathrm{D}_{7/2}$	44446.878 [18]	1616	3
			$3d^64p\ z\ ^4\mathrm{F}_{7/2}$	44753.799 [18]	1701	141
			$3d^64p\ z\ ^8\mathrm{P}_{7/2}$	54490.2 [19]	1719	-179
			$3d^64p\ z\ ^4\mathrm{G}_{7/2}$	60956.82 [19]	1724	6
			$3d^64p\ z\ ^4\mathrm{H}_{7/2}$	61156.835 [18]	1780	-86
			$3d^64p\ y\ ^4\mathrm{D}_{7/2}$	61726.078 [18]	1342	-51
			$3d^64p\ y\ ^4\mathrm{F}_{7/2}$	62065.528(3) [11]	1110	48
			$3d^64p\ y\ ^6\mathrm{P}_{7/2}$	62171.625(3) [11]	1002	141

Table 4. Same as Tables 1 - 3; Z = 28 - 32

Z	Atom/Ion	Ground state	Upper states	ω_0	q_1	q_2
28	Ni II	$3d^9\ ^2D_{5/2}$	$3d^84p\ z^2G_{7/2}$	56371.41 [18]	-134	0
			$3d^84p\ z\ ^2F_{7/2}$	57080.373(4) [16]	231	0
			$3d^84p\ z\ ^2D_{5/2}$	57420.013(4) [16]	-1188	0
			$3d^84p\ z\ ^2F_{5/2}$	58493.071(4) [16]	654	0
			$3d^84p\ z\ ^2D_{3/2}$	58705.94 [18]	275	0
			$3d^84p\ y\ ^2F_{5/2}$	67694.63 [18]	-1329	0
			$3d^84p\ y\ ^2F_{7/2}$	68131.22 [18]	-1158	0
			$3d^84p\ y\ ^2D_{3/2}$	68154.29 [18]	-585	0
			$3d^84p\ y\ ^2D_{5/2}$	68735.99 [18]	403	0
			$3d^84p\ z\ ^2P_{3/2}$	68965.66 [18]	266	0
			$3d^84p\ x\ ^2D_{5/2}$	71720.82 [18]	-451	0
			$3d^84p\ x\ ^2D_{3/2}$	72375.40 [18]	-444	0
			$3d^84p\ y\ ^2P_{3/2}$	72985.67 [18]	-336	0
			$3d^84p\ x\ ^2F_{7/2}$	75917.64 [18]	-876	0
			$3d^84p\ y\ ^2G_{7/2}$	79823.05 [18]	-716	0
30	Zn II	$3d^{10}4s\ ^2S_{1/2}$	$3d^{10}4p\ ^2P_{1/2}$	48481.077(2) [16]	1445	66
			$3d^{10}4p\ ^2P_{3/2}$	49355.002(2) [16]	2291	94
32	Ge II	$4s^24p\ ^2P_{1/2}$	$4s^25s\ ^2S_{1/2}$	62403.027 [18]	-575	-16

corrections to the valence electron energies and wave functions and screening of the electron-electron interaction by the core electrons.

- Diagonalization of the effective Hamiltonian for the valence electrons (the configuration interaction method).

The results are presented in the Tables 1 to 4.

We see that some lines have a large increase in frequency when α increases (e.g. lines with large positive q_1 coefficients – "positive shifters" – like FeII and ZnII), some lines have a large decrease in frequency (e.g. lines with large negative q_1 coefficients – "negative shifters" – like CrII) and there are "anchor" lines which are not sensitive to a variation of α (e.g. lines with small q_1 like MgI, MgII, AlII, AlIII, SiII).

3 Results of Observations

In this section we follow the work in [3]. All our QSO (quasar) spectra used in this work were obtained at the Keck I 10m telescope. The measurements of α-variation are based on two samples of data which loosely separate into two redshift régimes. The low-redshift sample ($\bar{z} = 1$) contains 28 absorption systems in the spectra of 17 QSOs with MgII and FeII lines. Full details of the reduction process are given in [25]. The absorbers in this sample lie in the range $0.5 < z < 1.8$ and so the useful transitions here are the five Iron lines, FeII λ2344–λ2600, and the Magnesium transitions, MgII λ2796 and λ2803. The MgII

lines have small q_1 coefficients and so act as anchors against which the larger FeII shifts can be measured.

The high redshift ($\bar{z} = 2.1$) sample contains 21 systems in the spectra of 13 QSOs. The absorbers in this sample lie in the range $0.9 < z < 3.5$ and contain absorption from some or all of the following species: SiII, NiII, ZnII, FeII and CrII lines. Full details of the reduction procedures can be found in [26].

Table 5. Statistics for the two subsamples and the sample as a whole. We give the average redshift, $\bar{z}$, for each sample and the number of data points, N, contributing to the weighted mean, $\langle \Delta\alpha/\alpha \rangle_{\rm w}$, and unweighted mean, $\langle \Delta\alpha/\alpha \rangle$ (in units 10^{-5}). We also give the significance of the deviation from zero and the reduced χ^2 when the weighted mean is taken as the model

Sample	$\bar{z}$	N	$\langle \Delta\alpha/\alpha \rangle_{\rm w}$	$\langle \Delta\alpha/\alpha \rangle$	Significance	$\chi^2_{\rm red}$
Low z	1.02	28	-0.75 ± 0.23	-0.76 ± 0.32	3.3σ	0.82
High z	2.12	21	-0.74 ± 0.28	-0.62 ± 0.36	2.7σ	0.77
Total	1.49	49	-0.75 ± 0.18	-0.70 ± 0.24	4.3σ	0.78

Our results are presented in Table 5. It shows the weighted mean (including statistical error bars), $\langle \Delta\alpha/\alpha \rangle_{\rm w}$, the unweighted mean, $\langle \Delta\alpha/\alpha \rangle$ and the significance level of the weighted mean for the low and high redshift samples, together with those statistics for the sample as a whole. We also include the value of the reduced χ^2, $\chi^2_{\rm red}$ (i.e. χ^2 per degree of freedom), for each sample where the model is taken to be a constant equal to $\langle \Delta\alpha/\alpha \rangle_{\rm w}$.

Our results show a 4.3σ variation in α over the redshift range $0.5 < z < 3.5$. We note that the weighted means do not differ significantly from the unweighted means for either sample. This indicates that we have not grossly underestimated the error bars on some small number of points, allowing them to dominate the overall weighted mean. Therefore, our results seem statistically self consistent.

To illustrate the distribution of $\Delta\alpha/\alpha$ over cosmological time, we plot our results in Fig. 1. The upper panel of Fig. 1 shows the raw values of $\Delta\alpha/\alpha$ as a function of fractional look-back time to the absorbing cloud using a flat Λ cosmology ($H_0 = 68$ kms^{-1}Mpc^{-1}, $\Omega_{\rm M} = 0.3$, $\Omega_\Lambda = 0.7$). The redshift scale is also given for comparison. The lower panel shows an arbitrary binning of the data such that all bins have equal number of points (7 bins $\times$ 7 points per bin = 49 points). We plot the weighted mean for each bin with the associated 1σ error bars. At low redshifts we see that $\Delta\alpha/\alpha$ is consistent with zero – an expected behaviour if indeed cosmological variation of α exists. It is tempting to overinterpret such a diagram but we do note that the results are consistent with a generally smooth evolution of α with redshift. Note that the last point contains large error bars. Therefore, this picture seems to be consistent with both oscillatory and monotonic time dependence of α.

We have also made a more complete analysis of two radio spectra initially treated in [21] to obtain constraints on $y \equiv g_p\alpha^2$. Assuming g_p to be constant,

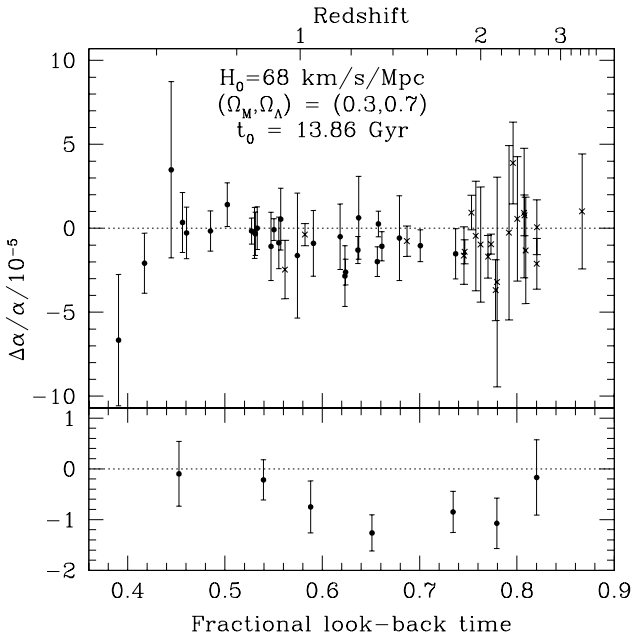

Fig. 1. $\Delta\alpha/\alpha$ versus fractional look-back time within the current popular cosmology. The upper panel shows our raw results and 1σ error bars: the dots represent the low redshift sample and the crosses mark the high redshift sample. Note that the high redshift sample does contain some lower redshift absorbers. The lower panel shows an arbitrary binning of our results: 7 bins $\times$ 7 points per bin = 49 points. The redshifts of the points are taken as the mean redshift of clouds within that bin and the value of $\Delta\alpha/\alpha$ is the weighted mean with its associated 1σ error bar

we find $\Delta\alpha/\alpha = (-0.1 \pm 0.1)10^{-5}$ and $\Delta\alpha/\alpha = (-0.2 \pm 0.2)10^{-5}$ at $z = 0.25$ and 0.68 respectively. If we note the low redshift points in the lower panel (binned data) of Fig. 1 then we see that our results are also consistent with the two radio points.

3.1 Systematic Errors?

The statistical error in our result is now small and so our attention must turn to possible systematic errors. The work [20] considers this aspect of the problem in great detail and so we present only the main points here.

To explain our results in terms of an effect other than real variation of α, such an effect must be capable of mimicking an non-zero average value of $\Delta\alpha/\alpha$ for both the high and low redshift samples alike. The low redshift sample (MgII/FeII systems only) is most sensitive to systematic effects since a non-zero $\Delta\alpha/\alpha$ can be mimicked by a slight 'stretching' or 'compression' of the spectrum relative to the ThAr calibration frames. This is due to the fact that all the FeII lines have

large and positive q_1 coefficients and all lie to the blue of the MgII anchors. A negative $\Delta\alpha/\alpha$ can be mimicked by a slight decrease in the separation between the MgII and FeII lines, that is, a slight compression of the spectrum. On the other hand, the high redshift sample is particularly insensitive to such simple forms of systematic error. Since the high redshift sample contains transitions of many different species, all with various magnitudes and signs of q_1 coefficients, it is unlikely that it is greatly effected by systematic effects.

We have considered a broad range of potential systematic errors. Most of these can be excluded with simple arguments. However, some require further consideration and others require a detailed analysis. These include the following: laboratory wavelength errors, wavelength miscalibration, atmospheric dispersion effects, unidentified interloping transitions, intrinsic instrumental profile variations, positioning of absorption features on different echelle orders, spectrograph temperature variations, heliocentric velocity corrections, isotopic ratio and/or hyperfine structure variations and large scale magnetic fields. We have conducted extensive numerical tests to quantify the effect (if any) of the first six of these on our measurements of $\Delta\alpha/\alpha$ and have reliably excluded all but one, atmospheric dispersion effects. We have yet to properly quantify this effect but it can only have shifted $\Delta\alpha/\alpha$ in the positive sense; removing this effect from our data will yeild a more significant result. We have excluded the rest of the above effects with more general calculations and arguments.

We have also carried out other tests to search for a simple, unknown systematic effect. For example, it is unlikely that such an effect will be able to mimick the very specific q_1 dependence of the various lines: spurious effects do not "know" the magnitude and sign of the relativistic corrections to the transition frequencies. Thus, if we remove the transitions with large positive or negative q_1 coefficients from our fit and find new values for $\Delta\alpha/\alpha$, then we expect the two values to differ in sign if the line shifts are caused by some simple systematic effect. We have conducted such a test on the high redshift sample since it contains a subset of 12 systems in which we observe at least one anchor line, at least one transition with a large positive q_1 co-efficient and at least one with a large negative q_1 co-efficient. The results for $(\Delta\alpha/\alpha)$ are the following:

- No lines removed (actually, we do remove any lines that have "mediocre" shifts as to clearly deliniate the three different types of transitions)
  $(-1.31 \pm 0.39) \times 10^{-5}$
- The anchor lines removed (with absolute value of q_1 less than 300 cm^{-1})
  $(-1.49 \pm 0.44) \times 10^{-5}$
- The positive shifters removed (with $q_1 > 1000$ cm^{-1})
  $(-1.54 \pm 1.03) \times 10^{-5}$
- The negative shifters removed (with $q_1 < -1000$ cm^{-1})
  $(-1.41 \pm 0.65) \times 10^{-5}$

Thus, we find consistent values for the average values of $\Delta\alpha/\alpha$ both before and after the line removal. The interpretation that the line shifts we observe are caused by a varying α seems robust.

We also removed individual lines and all lines of an ion to test for possible effects of unknown line blending, change of isotopic ratio and laboratory wavelength errors.

From the above analysis we can conclude that if our results are due to some effect other than real variation in α, then this will only be revealed with further independent observations.

Acknowledgments

The works described in this review have been performed with J.D. Barrow, C.W. Churchill, M.J. Drinkwater, J.X.Prochaska, and A.M. Wolfe. We are very grateful to Ulf Griesmann, Sveneric Johansson, Rainer Kling, Richard Learner, Ulf Litzén, Juliet Pickering and Anne Thorne for conducting laboratory wavelength measurements especially for the present work and for communicating their results prior to publication. We would also like to thank Gillian Nave for very helpful communications.

References

1. V.A. Dzuba, V.V. Flambaum, J.K. Webb: Phys. Rev. Lett. **82**, 888 (1999); Phys. Rev. A**59**, 230 (1999); Phys. Rev. A, in press
2. J.K. Webb, V.V. Flambaum, C.W. Churchill, M.J. Drinkwater, and J.D. Barrow: Phys. Rev. Lett. **82**, 884 (1999)
3. J.K. Webb, M.T. Murphy, V.V. Flambaum, V.A. Dzuba, C.W. Churchill, J.X.Prochaska, A.M. Wolfe and J.D. Barrow: submitted to Phys. Rev. Lett.; M.T. Murphy, J.K. Webb, V.V. Flambaum, C.W. Churchill, J.X. Prochaska, A.M. Wolfe, and J.D. Barrow: submitted to Mon. Not. Roy. Ast. Soc.
4. W. Marciano: Phys. Rev. Lett. **52**, 489 (1984); J. D. Barrow: Phys. Rev. D, **35**, 1805 (1987)
5. T. Damour, and A. M. Polyakov: Nucl. Phys. B **423**, 596 (1994)
6. J. Bachall, M. Schmidt: Phys. Rev. Lett. **19**, 1294(1967)
7. D. A. Varshalovich, V. E. Panchuk, A. V. Ivanchik: Astron. Lett. **22**, 6 (1996)
8. D. A. Varshalovich and A. Y. Potekhin: Space Science Review, **74**, 259 (1995)
9. U. Litzén, J. W. Brault, A. P. Thorne: Phys. Scr. **47**, 628 (1993)
10. G. Nave , R. C. M. Learner, A. P.Thorne, C. J. Harris: J. Opt. Soc. Am. B **8,** 2028 (1991)
11. S. Johansson: Private communication
12. R. E. Drullinger, D. J. Wineland, J. C.Bergquist: Appl. Phys. **2**, 365 (1980)
13. W. Nagourney , H. G. Dehmelt: Bull. Am. Phys. Soc. 26, 805 (1981)
14. J. C. Pickering, A. P. Thorne, J. K. Webb: Mon. Not. Roy. Ast. Soc. **300**, 131 (1998)
15. U. Griesmann, R. Kling, 2000: Submitted to Astrophys. J. Lett.
16. J. C. Pickering, A. P. Thorne, J. E. Murray, U. Litzén, J. K. Webb, 2000: submitted to Mon. Not. Roy. Ast. Soc.
17. J. Sugar, C. Corliss: 1985, J. Phys. Chem. Data, **14**, Supplement No 2
18. D. C. Morton: Astrophys. J. Supl. **77**, 119 (1991)

19. C. E. Moore: 1958, *Atomic Energy Levels*, Natl. Bur. Stand. (US), Circ. No. 467 (Washington), vol. **1**
20. M.T. Murphy, J.K. Webb, V.V. Flambaum, C.W. Churchill, J.X. Prochaska: to be submitted to Mon. Not. Roy. Ast. Soc.
21. M.J. Drinkwater, J.K. Webb, J.D. Barrow and V.V. Flambaum: Mon. Not. R. Astron. Soc. **295**, 457 (1998)
22. I. I. Sobelman: *Introduction to the Theory of Atomic Spectra*, Nauka, Moscow, (1977) (Russian)
23. V. A. Dzuba, V.V. Flambaum, O.P. Sushkov: J. Phys. B **16**, 715 (1983); V. A. Dzuba, V. V. Flambaum, P. G. Silvestrov, and O. P. Sushkov: J. Phys. B **20**, 1399 (1987)
24. V. A. Dzuba, V. V. Flambaum, M. G. Kozlov: JETP Lett. **63**, 882 (1996); Phys. Rev. A **54**, 3948 (1996)
25. C. W. Churchill: Lick Technical Report #74, 1995; C. W. Churchill: 'The low ionization content of intermediate redshift galaxies', PhD. thesis, UC Santa Cruz, 1997; C. W. Churchill, J. R. Rigby, J. C. Charlton, S. S. Vogt: Astrophys. J. Supl. **120**, 51 (1999)
26. J. X. Prochaska, A. M. Wolfe: Astrophys. J. **470**, 403 (1996); Astrophys. J. **474**, 140 (1997); Astrophys. J. Supl. **121**, 369 (1999)